



Data Article

Data for “Folding and Deploying Identical Thick Panels with Spring-loaded Hinges”

Jingyi Yang, Yunlan Zhang, Manolis N. Chatzis, Zhong You*

Department of Engineering Science, University of Oxford, Parks Road, Oxford OX1 3PJ, United Kingdom

ARTICLE INFO

Article history:

Received 1 March 2022

Revised 27 May 2022

Accepted 10 June 2022

Available online 16 June 2022

Dataset link: [Measurement of spring stiffness and damping \(Original data\)](#)

Keywords:

Quasi-static measurement

Free-vibration test

System identification

State-space estimation

Collision-free deployment

ABSTRACT

This article provides supplementary information for the manuscript “Folding and Deploying Identical Thick Panels with Spring-loaded Hinges” (Yang et al. 2022), in which collision-free deployments of a multiple degree-of-freedom (DoF) system are realized by using elastic hinges. This article characterizes two important parameters of such hinges, namely, the spring stiffness and the damping coefficient. The spring stiffness was acquired through quasi-static measurement of torque. A test rig consisting of rotary tables and strain gauges was developed for this purpose. The damping coefficient of the hinge was acquired by analyzing the responses of five free-vibration tests on a rotational mass-spring system. The time history of the response was processed, followed by system identification through the state-space estimation. Apart from the properties of the elastic hinges, the other system properties that were used for the simulations and the physical prototypes in (Yang et al. 2022) were detailed in this article. With these parameters, deployments with and without collisions were demonstrated through videos (V1, V2, and V3).

Crown Copyright © 2022 Published by Elsevier Inc.

This is an open access article under the CC BY-NC-ND license (<http://creativecommons.org/licenses/by-nc-nd/4.0/>)DOI of original article: [10.1016/j.eml.2022.101637](https://doi.org/10.1016/j.eml.2022.101637)

* Corresponding author.

E-mail address: zhong.you@eng.ox.ac.uk (Z. You).Social media: [@JYang25871602](#) (J. Yang), [@YunlanZhang](#) (Y. Zhang)<https://doi.org/10.1016/j.dib.2022.108388>2352-3409/Crown Copyright © 2022 Published by Elsevier Inc. This is an open access article under the CC BY-NC-ND license (<http://creativecommons.org/licenses/by-nc-nd/4.0/>)

Specifications Table

Subject	Aerospace engineering
Specific subject area	Deploying solar panels and reflectarray antennas with spring-loaded hinges.
Type of data	Table Graph Figure Video
How the data were acquired	The torque of a spring was acquired through Omega TQ202 Series Reaction Torque Sensor and its corresponding angle of rotation was measured by two 60 mm × 60 mm Standa Rotary Tables. The damping of the hinge was acquired through free-vibration tests whose responses were recorded by accelerometers – PCB Piezotronics Model 393B04. The deployments of the prototypes were recorded by PHOTRON FASTCAM SA-X2 camera with a motion capture rate of 1000fps.
Data format	Raw, Filtered, and Analyzed
Description of data collection	A dataset containing two files was published in Mendeley repository. One file shows the torque versus angle of rotation of a torsional spring, which can be used to reproduce the stiffness of a torsional spring as shown in Fig. 1. The other one is the raw data for the free-vibration response of a mass-spring system measured by accelerometers. Fig. 4 was plotted based on that, which can be then used to calculate the damping coefficient of the elastic hinge. Regarding the spring stiffness, the output voltages of the two torsion gauges were recorded in an excel spreadsheet after every increment in the angle of rotation of the spring. Regarding the damping, the time histories of the free-vibration responses were sent to a PXI system (National Instruments PXIe-1082) with a sample rate of 200 Hz, which was then visualised through LabVIEW.
Data source location	<ul style="list-style-type: none">• Institution: University of Oxford• City/Town/Region: Oxfordshire• Country: U.K.• Latitude and for collected samples/data: 51.7520° N, 1.2577° W
Data accessibility	Repository name: Mendeley Data identification number (permanent identifier, i.e. DOI number): 10.17632/fnw2jrwwhx.1 Direct link to the dataset: https://data.mendeley.com/datasets/fnw2jrwwhx/1
Related research article	J. Yang, Y. Zhang, M.N. Chatzis, Z. You, "Folding and Deploying Identical Thick Panels with Spring-loaded Hinges", submitted to <i>Extreme Mechanics Letters</i> .

Value of the Data

- This article provides data for the manuscript “Folding and Deploying Identical Thick Panels with Spring-loaded Hinges” [1]. By characterising the spring-loaded hinges through experiments, the linear spring-viscous damper model used for modelling the hinge in the manuscript is validated.
- Besides, the data can be useful to engineers who aim to deploy a multiple-DoF system such as a solar array in space without using motorising actuators. If a hinge with the same mechanical properties was used everywhere to connect adjacent panels, collisions resulted. Employing the elastic hinges with different properties, the system was deployed from a compact volume to a flat surface without collision.
- The data summarising the system properties is relevant to researchers who wish to conduct dynamic simulations of a multibody system driven by elastic hinges.
- Furthermore, the approaches for acquiring the data can be used to characterise other elastic hinges, such as the flexure hinges manufactured by soft polymeric materials.

1. Data Description

Tests had been conducted to measure the spring stiffness of two torsional springs that were used to deploy the panels. The required torque to generate their corresponding angles of rotation were plotted in Fig. 1. The data points of the two springs were then linearly fitted with gradients of 0.10 Nm/rad for spring k_1 and 0.07 Nm/rad for spring k_2 , respectively, which were regarded as their respective stiffness.

Five free-vibration tests had been conducted and the natural frequency and its corresponding damping ratio were recorded in each test. After that, the damping coefficient c of the elastic hinge could be obtained by

$$c = \zeta c_c, \quad (1a)$$

and

$$c_c = 2I\omega_n \quad (1b)$$

where c_c is the critical damping coefficient of the system, and $I = 0.0051 \text{ kg}\cdot\text{m}^2$ is the moment of inertia of the aluminium mass block rotating about the hinges. Since four elastic hinges were connecting the mass block to the frame (the experiment setup is detailed in the next section), the damping coefficient of each elastic hinge was calculated as $c = 2I\omega_n\zeta/4$. Table 1 summarises the system properties obtained from five tests, whose first three columns are data for

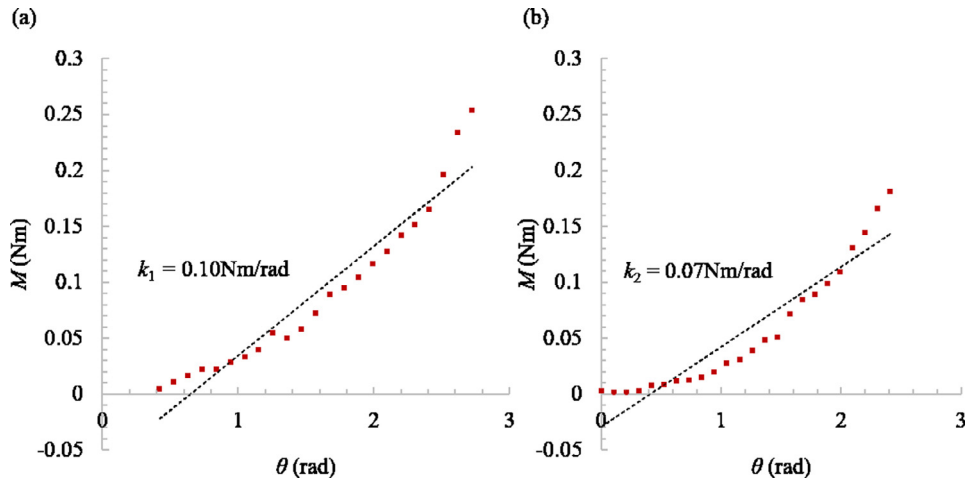


Fig. 1. Moment and rotational angle relationship of (a) spring k_1 , and (b) spring k_2 .

Table 1

Summary of the frequency, natural frequency, damping ratio, and the damping coefficient of the elastic hinges with stiffness 0.10 Nm/rad.

Test	Frequency f (Hz)	Natural frequency ω_n (rad/s)	Damping ratio ζ	Damping Coefficient c (Nm-s/rad)
1	2.425	15.237	0.111	0.0043
2	2.462	15.467	0.115	0.0045
3	2.642	16.598	0.100	0.0042
4	2.440	15.332	0.101	0.0039
5	2.516	15.811	0.109	0.0044
AVG*	2.497	15.689	0.107	0.0043
SD**	0.088	0.553	0.007	0.0002

* AVG is the abbreviation for average;

** SD is the abbreviation for standard deviation.

Table 2
Dimensions and physical properties of a small rigid panel.

Panel length l (mm)	50
Panel width w (mm)	40
Panel thickness t (mm)	6
Panel density ρ (kg/m ³)	547

Table 3
System properties in the simulations.

Initial hinge angle α_i (rad)	0.999π
Final hinge angle α_f (rad)	0
Contact stiffness k_s (Nm/rad)	10^6
Contact damping c_s (Nm.s/rad)	1
Cut joint stiffness k_M k_N (N/m)	10^8
Cut joint damping c_M c_N (Ns/m)	10

four hinges in parallel, and the last column lists the calculated damping coefficient for one hinge. The average damping coefficient is 0.0043 Nm.s/rad.

The dimensions and the density of the rigid panels that are used in the prototypes and the simulations are reported in Table 2. The panels were 3D printed by RAISE 3D N2 using Polylactic acid (PLA) material with 0.15 mm layer resolution and 5% honeycomb infill to obtain a reasonable precision while minimising the mass. The panel was then weighed on a scale and density was calculated from the ratio of the mass and volume of the panel.

When the same torsional spring with stiffness $k_1 = 0.1\text{Nm/rad}$ was used to connect the panels, the panels collided during the deployment process. A video V1 was recorded by PHOTRON FASTCAM SA-X2 camera with a motion capture rate of 1000fps. Therefore, an approach introduced in [1] was conducted and the dynamic simulations were initiated with the parameters introduced above and some other hinge properties listed in Table 3. A collision-free deployment was found by using different combinations of springs k_1 and k_2 at the hinges. A simulated result was presented in video V2, and a physical deployment was captured using the camera with the same settings in video V3. All videos are presented at 1/50 of their original speeds.

2. Experimental Design, Materials and Methods

The apparatus to test the stiffness of the torsional spring is shown in Fig. 2(a), which is a similar setup as described in [2]. Four threaded holes were drilled on the platform with equal distance away from the centre. To measure the angle of rotation of the torsional spring, a testing specimen was set up consisting of two rigid blocks connected by a rotational hinge that housed the spring. The two rigid blocks were mounted onto the platforms such that its mid-plane was passing through the geometric centre of each platform. The platforms were then connected to the shaft of a torsion gauge (Omega TQ202 Series Reaction Torque Sensor). The lower end of the platform fitted over the torsion gauge shaft and three grub screws were against three flat surfaces of the shaft of the torsion gauge to ensure that there would not be relative rotational motions between the platform and the shaft. Each gauge was wired to a 10v DC source and a voltmeter. When a torque was applied to its shaft, where a sensor plate was attached, an output voltage could be read from the voltmeter, indicating the magnitude of the applied torque. The torsion gauge on each side was then sat on a 60 mm × 60 mm Standa Rotary Table, respectively. The rotary table on the left-hand side was fixed to the ground through an aluminium block. The one on the right-hand side was mounted onto a carriage of the same height as the aluminium block that was moving linearly on two parallel rails. Therefore, the rigid block on the left-hand side could only rotate about the centre of its corresponding rotary table; while the one on the right-hand side had both rotating motion about the centre of its corresponding rotary table and

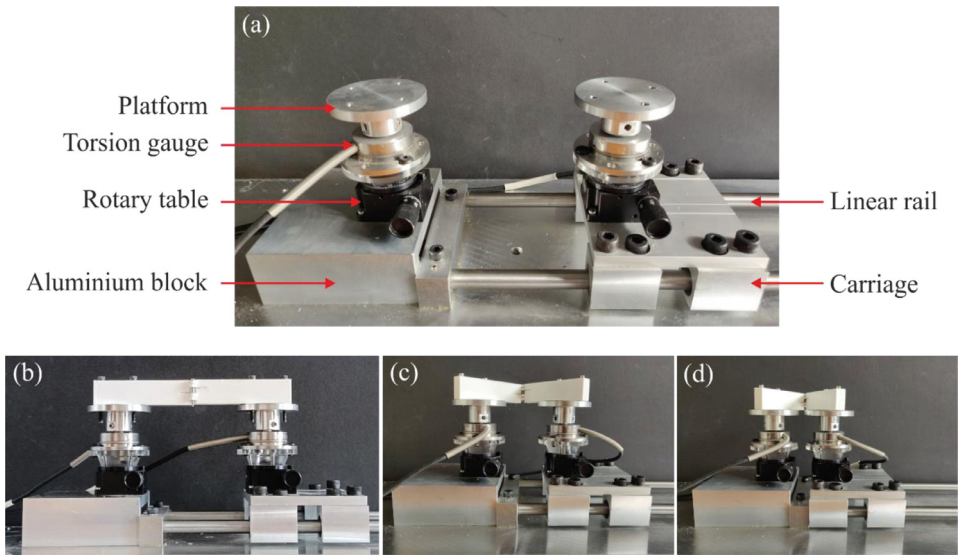


Fig. 2. (a) The apparatus to test the stiffness of torsional spring with all the parts labelled. The apparatus with test specimen mounted onto the platform in (b) initial position when no strain applied; (c) when it was in measurement; and in (d) the final state.

free linear motion along the rails. Between the rails and the carriage, bearings were installed to minimise friction when the carriage was travelling along the rails.

The experiment started when there was no strain in the torsional spring, where the angle of rotation of the spring is 0 rad, as shown in Fig. 2(b). The rotary tables were aligned at the best possible so the testing sample had as close to no moment applied. The rotation angles of the rotary tables were marked as 0 rad at both ends. Starting from 0 rad, a rotation was applied to the testing specimen by turning the knobs of the rotary tables at each end simultaneously in increments of 1 arcminute, which is $1/60\pi$. Driven by the rotary tables, the carriage moved closer to the aluminium block along the parallel rails as shown in Fig. 2(c). The torque incurred by the torsional spring was transferred to the strain gauges and indicated by the output voltages on the voltmeters. We then recorded the output voltages of the two gauges after every increment in an excel spreadsheet. The experiment continued until the distance between the aluminium block and the carriage became zero as shown in Fig. 2(d). Throughout the experiment, the output voltage on either voltmeter was ensured not to exceed 20 millivolts, which was 95% of the capacity of the torsion gauge. After the experiment, the voltage outputs were converted to bending moments according to calibration equations provided by the manufacturer's datasheet. In each increment, an average value of the bending moments at both ends was taken.

To measure the damping ratio of the elastic hinge, we conducted five free-vibration tests on a single Degree-of-Freedom (DoF) rotational system as shown in Fig. 3. The top mass block was fixed to an aluminium frame that was grounded. The bottom mass block, which weighed 0.98 kg, was allowed to rotate with respect to the top one resisted by four elastic hinges with the spring stiffness of 0.10 Nm/rad each. To acquire the free-vibration response of the system, two accelerometers (PCB Piezotronics Model 393B04) with sensitivities of 1005 and 998 mV/g were mounted onto the centres of the surfaces of the top and bottom mass blocks, respectively. The time histories of acceleration were sent to a PXI system (National Instruments PXIe-1082) with a sampling rate of 200 Hz, which then could be visualised through LabVIEW.

In each test, the bottom mass block was excited by an Impact Hammer (Impulshammer inkl. Kraftaufnehmer 8200) that resulted in an initial velocity of it. After each hammer struck, the responses of the frame and the mass block were recorded until the mass block came to a rest. An

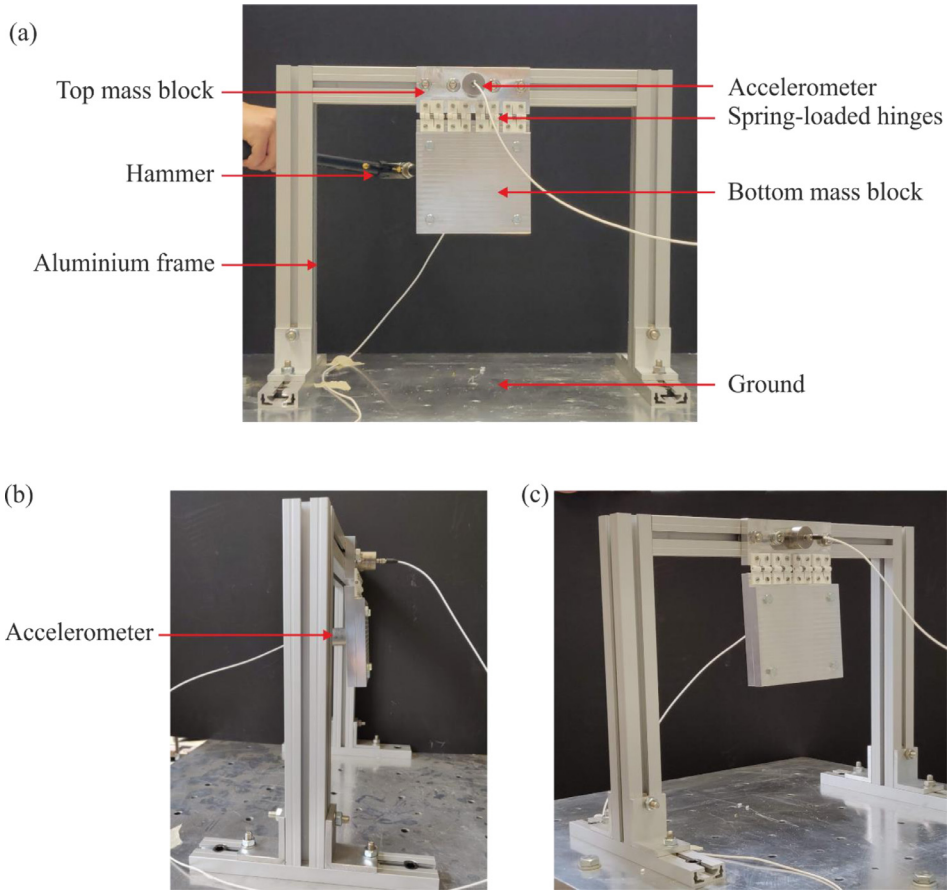


Fig. 3. The experimental setup for free vibration tests on a single-DoF rotational system with all parts labelled in its (a) front view, (b) side view, and (c) isometric view.

example is shown in Fig. 4 in which a decaying motion of the mass block and constant vibration of the frame can be observed. After processing the data through a highpass Butterworth filter [3], which eliminated low-frequency noise that was below 0.5 Hz, we carried out the system identification by estimating a state-space model of the system using the N4SID algorithm [4,5]. The frequencies and damping ratios corresponding to the identified state-space matrices were then calculated, e.g., as described in [6].

After dropping the first data points for which the hammer was still in contact with the mass block, the acceleration of the frame was used as an input signal, with the acceleration of the mass block used as an output signal. N4SID resulted in models of different state sizes from which the natural frequencies ω_n and the damping ratios ζ of the system were retrieved from the eigenvalues of the state matrix of the state-space model [7]. Typically, successful model orders were of the size of 6 resulting in 3 modes. For instance, the natural frequencies of the structure were calculated to be 15.2 rad/s, 238.8 rad/s, and 578.1 rad/s in one test. Only the smallest natural frequency and its corresponding damping ratio were recorded in each test as they described the vibration mode due to the rotation of the panel about the hinges. The larger natural frequencies and their corresponding damping ratio were not our interests as they appear to be associated with additional vibrational modes of the aluminium frame. The large

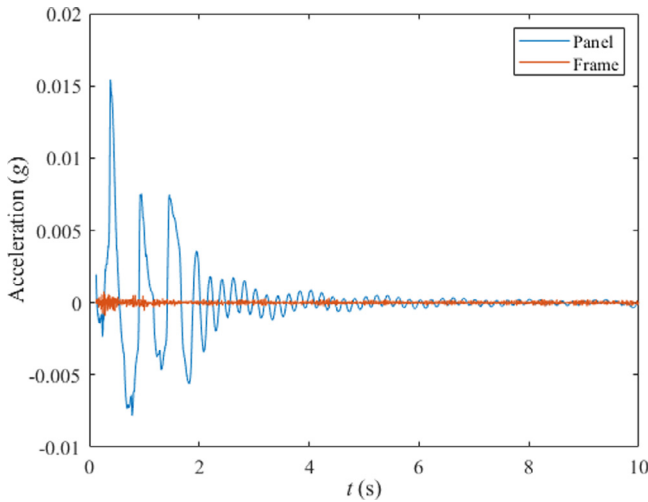


Fig. 4. The free vibration response of the torsional spring-mass system after a hammer strike. The amplitude was recorded as a magnitude of gravitational acceleration g .

separations between the identified modes also allowed to proceed in truncating to the first mode, which appears to describe the rigid rotation of the mass block about the elastic hinges.

Declaration of Competing Interest

The authors declare that they have no known competing financial interests or personal relationships that could have appeared to influence the work reported in this paper.

The authors declare the following financial interests/personal relationships which may be considered as potential competing interests:

Data Availability

Measurement of spring stiffness and damping (Original data) (Mendeley Data).

CRediT Author Statement

Jingyi Yang: Methodology, Data curation, Formal analysis, Writing – original draft; **Yunlan Zhang:** Data curation, Formal analysis; **Manolis N. Chatzis:** Investigation, Supervision, Writing – review & editing; **Zhong You:** Supervision, Writing – review & editing.

Acknowledgements

The authors would like to thank Professor Clive Siviour and his D.Phil student Mr Thomas Commins for borrowing us the PHOTRON high-speed camera and helping us with the settings. We would like to acknowledge Mr Clive Baker and Mr Duncan Constable for their help manufacturing the test specimen for the damping test. In addition, J. Yang would like to thank the Agency for Science, Technology and Research (A*STAR), Singapore, which is financially sponsoring her DPhil studies.

Supplementary Materials

Supplementary material associated with this article can be found in the online version at doi:[10.1016/j.dib.2022.108388](https://doi.org/10.1016/j.dib.2022.108388).

References

- [1] J. Yang, Y. Zhang, M.N. Chatzis, Z. You, Folding and deploying identical thick panels with spring-loaded hinges, *Extreme Mechanics Letters* 52 (2022) 101637, doi:[10.1016/j.eml.2022.101637](https://doi.org/10.1016/j.eml.2022.101637).
- [2] K.A. Seffen, S. Pellegrino, Deployment dynamics of tape springs, *R. Soc.* 455 (1999) 1003–1048.
- [3] C. Greene, “Butterworth filters,” version 1.3.0.0, MATLAB central file exchange, 2021. [Online]. Available: <https://www.mathworks.com/matlabcentral/fileexchange/38584-butterworth-filters>. Accessed December 14, 2021.
- [4] P. Van Overschee, B. De Moor, N4SID: subspace algorithms for the identification of combined deterministic-stochastic systems, *Automatica* 30 (1) (1994) 75–93.
- [5] L. Ljung, *System identification toolbox, The Matlab user's guide*, The MathWorks, 1988.
- [6] E. Reynders, System identification methods for (operational) modal analysis: review and comparison, *Arch. Comput. Methods Eng.* 19 (1) (2012) 51–124.
- [7] F.J. Cara, J. Juan, E. Alarcón, E. Reynders, G. De Roeck, Modal contribution and state space order selection in operational modal analysis, *Mech. Syst. Signal Process.* 38 (2) (2013) 276–298.